

# N-SLIT INTERFERENCE: FRACTALS IN NEAR-FIELD REGION, BOHMIAN TRAJECTORIES.

Valeriy I. Sbitnev\*

*B.P.Konstantinov St.-Petersburg Nuclear Physics Institute,  
Russ. Ac. Sci., Gatchina, Leningrad district, 188350, Russia.*

(Dated: January 10, 2023)

Scattering cold particles on an  $N$ -slit grating is shown to reproduce an interference pattern, that manifests itself in the near-field region as the fractal Talbot carpet. In the far-field region the pattern is transformed to an ordinary diffraction, where principal beams are partitioned from each other by  $(N - 2)$  weak ones. A probability density plot of the wave function, to be represented by a gaussian wavepacket, is calculated both in the near-field region and in the far-field one. Bohmian (geodesic) trajectories, to be calculated by a guidance equation, are superimposed on the probability density plot well enough. It means, that a particle, moving from a source to a detector, passes across the grating along a single bohmian trajectory through-passing one and only one slit.

Keywords: Gaussian wavepacket, near-field interference, far-field diffraction, Talbot carpet, fractal, bohmian trajectory, guidance equation

## I. INTRODUCTION.

Wave interference is a most impressive phenomenon be it induced by waves on water, acoustic waves, or electromagnetic ones - radio-waves, light waves,  $\gamma$ -radiation. Quantum-mechanical experiments deal with interference phenomena as well [1, 2]. A particular interest to these phenomena is due to problem of quantum computing [3], where interference can play an important role at manipulations with qubits. The interference effects in these cases are important in near-field region, i.e., in the vicinity of an interference grating. In this region complex wave interference shows very exotic patterns [2], named in literature as the Talbot carpets disclosing fractal-like structures. Fig. 1, for example, demonstrates the optical Talbot carpet for monochromatic light to be scattered on 4-slit grating. Henry Fox Talbot was first who observed in 1836 such an effect in a near-field region [23]. Most striking observation in Fig. 1 is existence of fractal structures, sizes of which are smaller than distance between slits.

As a distance from the slit grating to a detector increases the exotic near-field interference transforms to diffraction pattern observed in the far-field region to be described by a well-known

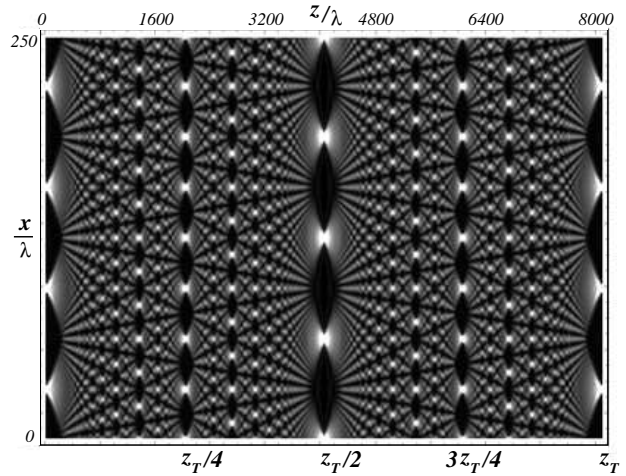


FIG. 1: The optical Talbot effect for monochromatic light, shown as a "Talbot Carpet", captured from <http://en.wikipedia.org/wiki/Talbot-effect>.

formula [4]

$$I(\zeta) = I_0(\zeta) \cdot \frac{\sin^2 \frac{N\zeta}{2}}{\sin^2 \frac{\zeta}{2}} \quad (1)$$

Function  $I_0(\zeta)$  is an envelope describing diffraction on a single slit and

$$\zeta = \frac{2\pi}{\lambda} d \sin(\theta)$$

is a phase shift of the waves emitted from two nearest slits, see Fig. 2. Observe that Eq. 1 is quite common formula. For example, it describes

\*Electronic address: valery.sbitnev@gmail.com

also revolution of spin of neutrons flying through an  $N$ -periodic magnetic field [5].

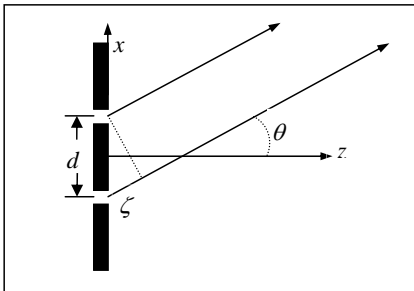


FIG. 2: Diffraction from two slits in far-field region:  $d$  is distance between the slits,  $\theta$  is deflection angle with respect to axis  $z$ , and  $\zeta$  is phase shift of wave rays emitted from the slits.

As was mentioned, interference effects in the near-field regions can be important with the point of view of quantum computing perspective. Theoretical study of the near-field interference by means of preparation of quantum mechanical models is the first step for an understanding of the quantum computing perspective. Gaussian wavepacket [6, 7] is a simplest model for studying  $N$ -slit grating interference. Sec. II deals with the Gaussian wavepacket and its Fourier transforms that give rise to emergence of complex, time-dependent, variance. In Sec. III we simulate interference by radiation of the Gaussian wavepackets from the  $N$ -slit grating. Their dispersion in the near-field region produces an interference pattern that manifests itself in a fractal organization of probability density of the wave function. As the detector is shifted in the far-field region the interference pattern transforms to diffraction pattern described by Eq. (1). In that region fractality disappears. Instead of this, principal maxima of radiation come into being. And they are partitioned by  $(N - 2)$  subsidiary maxima. Next, the problem is to understand, how does a particle pass through the  $N$ -slit grating up to a detector. David Bohm had revealed that the particle travels along a single optimal trajectory [8, 9], which is named in literature the bohmian trajectory. This approach together with calculation of trajectories is discussed in Sec. IV. Comparison of classical trajectories and bohmian is given in Sec. V, concluding

section. In this section we discuss the bohmian trajectories passing through a slit up to the detector, and waviness of the bohmian trajectories caused by exchange of virtual particles with vacuum that is tuned by de Broglie pilot-wave.

## II. GAUSSIAN WAVEPACKET AND ITS FOURIER TRANSFORMS.

As seen in Fig. 2, Eq. 1 results from computation of interference of cylindrical waves divergent from the slits. The waves in the vicinity of the slits are no cylindrical, in general. They have a complex form when transforming from a plane wave to cylindrical one. For the sake of simplicity, we suppose that slit borders are fuzzy under Gauss distribution, and a wave from the slit is approximated by the Gaussian wavepacket [6, 10]

$$\varphi_0(x) = \sqrt[4]{\frac{1}{2\pi\sigma^2}} \exp\left\{-\frac{(x-x_0)^2}{4\sigma^2}\right\}. \quad (2)$$

Observe that  $\varphi_0^2(x) = p(x)$  is the probability density distribution with a mean  $x_0$  and variance  $\sigma^2 \geq 0$ .

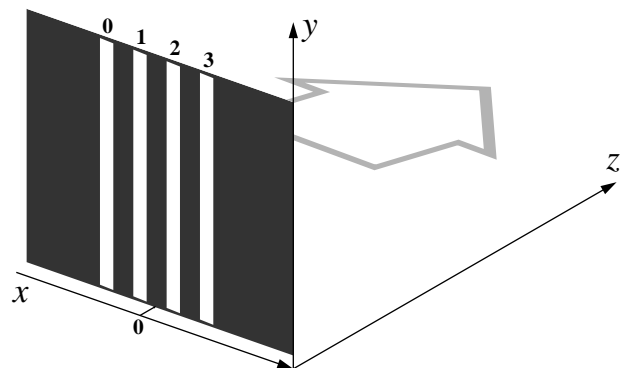


FIG. 3: Interference experiment in a cylindrical geometry - the grating is placed in the plane  $(x, y)$  and slits go along the axis  $y$ . Gray arrow points direction of wave radiation.

The wavepacket 2 disperses as it moves away from the slit to a region pointed out by grey arrow in Fig. 3. Let us express this wavepacket by superposition of harmonic waves  $\exp\{-2\pi i k x_0\}$  with wave number  $k$  ranging from  $-\infty$  to  $\infty$ . To that end, we execute the Fourier transform

$$\begin{aligned}
F_x[\varphi_0(x)](k) &= \sqrt[4]{\frac{1}{2\pi\sigma^2}} \int_{-\infty}^{\infty} \exp\left\{-\frac{(x-x_0)^2}{4\sigma^2}\right\} \exp\{-2\pi\mathbf{i}kx\} dx \\
&= \sqrt[4]{8\pi\sigma^2} \exp\{-\pi^2 4\sigma^2 k^2\} \exp\{-2\pi\mathbf{i}kx_0\} = \Phi_0(k).
\end{aligned} \tag{3}$$

The function  $\Phi_0(k)$  is seen to be a harmonic wave  $\exp\{-2\pi\mathbf{i}kx_0\}$  having an amplitude

$$A(k) = \sqrt[4]{8\pi\sigma^2} \exp\{-\pi^2 4\sigma^2 k^2\}. \tag{4}$$

As we move off from the slit, the wave components  $\Phi_0(k)$  spread along axis  $x$  differently for different  $k$ . Let the dispersed wave component be  $\Phi_0(k) \exp\{-\mathbf{i}2\pi k \cdot \pi x\}$ . Additional factor  $\pi$  scales the dispersion along axis  $x$ . Observe that  $x = vt$  and a speed of the shift along

axis  $x$  is  $v = \hbar k/m$ . Here  $\hbar$  is the reduced Planck constant,  $m$  is a particle mass. As far as  $2\pi k \cdot k = (2\pi k)^2/2\pi$ , a shifted wave component is

$$\Phi_0(k) \exp\left\{-\mathbf{i}(2\pi k)^2 \frac{\hbar}{2m} \cdot t\right\}. \tag{5}$$

Let us now execute the inverse Fourier transform of the function 5

$$\begin{aligned}
F_k \left[ \Phi_0(k) \exp\left\{-\mathbf{i}(2\pi k)^2 \frac{\hbar}{2m} \cdot t\right\} \right] (x) \\
&= \sqrt[4]{8\pi\sigma^2} \int_{-\infty}^{\infty} \exp\{-\pi^2 4\sigma^2 k^2\} \exp\left\{-\mathbf{i}(2\pi k)^2 \frac{\hbar}{2m} \cdot t\right\} \exp\{2\pi\mathbf{i}k(x-x_0)\} dk \\
&= \sqrt[4]{\frac{2}{4\pi\sigma_t^2}} \exp\left\{-\frac{(x-x_0)^2}{4\sigma\sigma_t}\right\} = \phi(x, x_0, t).
\end{aligned} \tag{6}$$

Here

$$\sigma_t = \sigma \left( 1 + \mathbf{i} \frac{\hbar}{2m} t \cdot \sigma^{-2} \right) \tag{7}$$

is a time-dependent deviation. It should be noted, that it is a complex variable of time  $t$ . Getting ahead, we can say that this complex variable [6, 7] determines fractal pattern in the near-field region. Observe that at  $t = 0$  we have  $\sigma_{t=0} = \sigma$  and the function 6 comes to  $\phi_0(x)$ .

### III. RADIATION FROM $N$ -SLIT GRATING.

The function 6 is not yet a wave function since it contains no a term describing its translation forward the region, as shown by grey arrow in Fig. 3. The term describing such a translation along axis  $z$  is represented by a factor  $\exp\{\mathbf{i}\omega t - \mathbf{i}k_z z\}$ . Here  $E = \hbar\omega$  is a particle energy and  $p_z = \hbar k_z$  is its momentum along axis  $z$ . The wave function, in such a case, reads

$$\Psi(x, x_0, z) = \phi(x, x_0, t) \exp\{\mathbf{i}\omega t - \mathbf{i}k_z z\} = \sqrt[4]{\frac{2}{4\pi\sigma_t^2}} \exp\left\{-\frac{(x-x_0)^2}{4\sigma\sigma_t}\right\} \exp\{\mathbf{i}\omega t - \mathbf{i}k_z z\} \tag{8}$$

A velocity along axis  $z$  is  $v_z = p_z/m = \hbar k_z/m$ . So, we can express time  $t$  in the function 8 via

variable  $z/v_z$ . Therefore, arguments in the func-

tion  $\Psi(x, x_0, z)$  do not contain  $t$ .

Putting the frame of axis  $x$  in center of the slit grating, containing  $(N + 1)$  slits,  $(n = 0, 1, 2, \dots, N)$ , as shown in Fig. 3, we find that position of  $n^{\text{th}}$  slit is  $x_0 = (n - N/2)d$ . Here distance  $d$  is period of the grating. Superposition of the waves 8 emitted by all  $(N + 1)$  slits reads

$$|\Psi(x, z)\rangle = \frac{1}{N+1} \sum_{n=0}^N \Psi\left(x, \left(n - \frac{N}{2}d\right), z\right). \quad (9)$$

Probability density

$$p(x, z) = \langle \Psi(x, z) | \Psi(x, z) \rangle \quad (10)$$

is an observable. Fig. 4 shows the probability density  $p(x, z)$  which is calculated within a transient region from the near-field region to the far-field ones. The grating contains four slits. It should be noted, that coordinate  $z$  in this figure begins from a value that is slightly more than zero. The whole point is that the wave function at  $z = 0$  has singularities located on the slits.

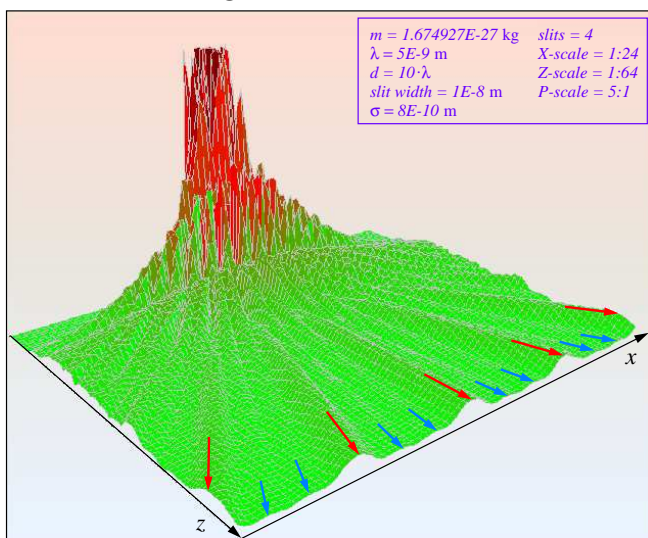


FIG. 4: Diffraction pattern in a transient region,  $(x; z) \in ((0 \dots 1.4 \times 10^{-6}); (5 \times 10^{-8} \dots 3.8 \times 10^{-6}))$  m, from near-field to far-field ones. Red arrows point out to directions of radiation along the principal peaks. Blue arrows point out to directions of weak radiation along the subsidiary maxima.

Here we have simulated neutron scattering on the slits, with the neutrons having a wavelength  $\lambda = 5\text{nm}$ . Kinetic energy of the neutrons is about  $5.25 \times 10^{-24}$  J. It means, that the neutrons are very cold [24], i.e., temperature of the neutrons is about  $T = E/kB \approx 0.38$  K. Here

$kB \approx 1.38 \times 10^{-23}$  JK $^{-1}$  is the Boltzmann constant.

Fig. 4 demonstrates diffraction pattern in a transition region from the near-field region to the far-field one. Red arrows point out to the principal maxima. And blue arrows point out to the subsidiary maxima. Alternation of the principal maxima and subsidiary ones is described by Eq. 1. Parameters  $\zeta$  and  $I_0$ , in this case, have the following forms [4]

$$\zeta(x, z) = xd \frac{m\hbar(z/v_z)}{D(z)} \quad (11)$$

and

$$I_0(x, z) = \sqrt{\frac{1}{\pi}} \frac{m\sigma}{\sqrt{D(z)}} \exp\left\{-\frac{2m^2\sigma^2x^2}{D(z)}\right\}, \quad (12)$$

where denominator  $D(z)$  is as follows

$$D(z) = m^2\sigma^4 + \hbar^2(z/v_z)^2/4. \quad (13)$$

Here  $(z/v_z) = t$  is a flight time along the path length  $z$ . Diffraction curve 1, at substituting terms  $\zeta$  and  $I_0$  by functions 11-12, has been calculated in the far-field region,  $z = 0.004$  m, is shown in Fig. 5. Circles in this figure relate to results simulated by means of the Gaussian wavepacket.

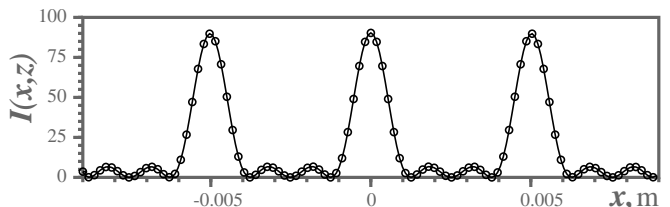


FIG. 5: Diffraction in the far-field region,  $z = 0.004$  m. Cross-section of the diffraction pattern (see previous figure) is displayed by circles. Solid curve shows the same cross-section calculated by the diffraction formula 1 with parameters  $\zeta$  and  $I_0$  defined in Eqs. 11 and 12.

Turn back to Fig. 4. In order to show the diffraction pattern in the far-field region, we have coarsen resolution of the probability density distribution. For this reason, we see a rough pile-up of maxima in the near-field region. Fig. 6 shows the same pattern at more detailed resolution in the near-field region. One can see, the probability density distribution increases catastrophically nearby the slits. At some distance from the

slits, their radiations are superimposed with each other. Such a superposition manifests itself by emergent peaks. The peaks near the slits seem short. And they become longer, as a look moves from the slits to the far-field region. As soon as the detector is shifted to the far-field region, the peaks are transformed to typical diffraction rays going away to infinity.

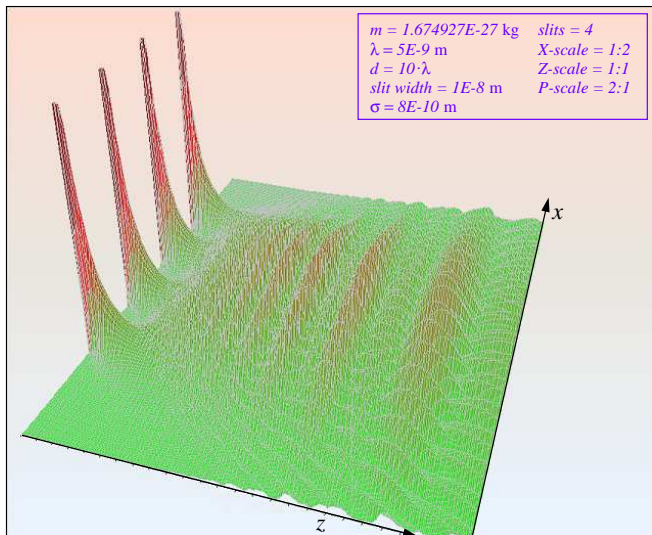


FIG. 6: Diffraction pattern in the near-field region,  $(x, z) \in ((0 \dots 3 \times 10^{-7}); (8 \times 10^{-10} \dots 2 \times 10^{-7}))$  m. Ripples of the probability density lengthen as distance to the N-slit sources is increased.

#### IV. DENSITY DISTRIBUTION PLOT AND BOHMIAN TRAJECTORIES.

Let us project the density distribution  $p(x, z)$  to the plane  $(x, z)$ . Fig. 7 demonstrates this projection in grey palette. Dark places show maximal values of  $p(x, z)$ , black patches, in particular, side with the slits. Light places relate to minimal values. Fractality in the interference pattern are well visible when passing from the slit sources to the right edge of the figure.

Violet curves traced in the upper part of the figure depict bohmian trajectories. Finding the trajectories is based on variation of the action integral [11], which leads to the principle of least action. A general formula computing the bohmian trajectory [7, 12] the guidance equation [13], reads:

$$v_x = \dot{x} = \frac{\hbar}{m} \Im \left( |\Psi(x, z)\rangle^{-1} \nabla |\Psi(x, z)\rangle \right) \quad (14)$$

As a result, we can find a current position of the particle by the following formulas:

$$\begin{cases} x(t) = x_0 + \int_0^t v_x d\tau, \\ z(t) = z_0 + v_z \cdot t. \end{cases} \quad (15)$$

The velocity along  $z$  is  $v_z = \hbar k_z / m$ . It stems from the term  $\exp i\omega t - \mathbf{i}k_z z$  as adopted before, see Eq. 8.

Velocity  $v_x$  is seen from Eq. 14 to be (a) proportional to gradient of the wave function; and (b) inversely proportional to the same wave function. It means: (a) a trajectory undergoes greatest variations in parts, where the wave function demonstrates slopes; and (b) the trajectory avoids areas, where the wave function tends to zero. Violet wavy curves in Fig. 7 manifest themselves the above properties well enough. One can see, the wavy curves group predominantly in dark-grey spots and avoid white spots. In extreme cases, the trajectories traverse the white spots almost transversally.

Does this bohmian trajectory pattern relate to the many-worlds theory? Answer is negative [13, 14]. For that aim, let us scatter particles on the N-slit grating by single-piece. Let a single particle pass, for example, the central slit nearby the top border. As is shown in Fig. 7, the particle scatters to a direction pointed out by blue arrow  $a$ . Next, the particle goes on a wavy stream and follows to a place pointed out by blue arrow  $b$ . Here we suppose that, movement of the particle submits to the principle of least action. Therefore, a number of problems arises right now. The first problem arising here is as follows: what is cause which forces the particle to change its own direction in the vicinity of point  $a$ ? And the second problem is: what is cause which forces the particle to perform wavy motions? We confirm that, any experimental setup for a quantum mechanical experiment is, in fact, the quantum instrument. The setup contains, in our case, N-slit grating with its parameters fitted for a wavelength of the particle. Boundary conditions of the setup determine the wave function on the edges. In whole, the experimental setup deter-

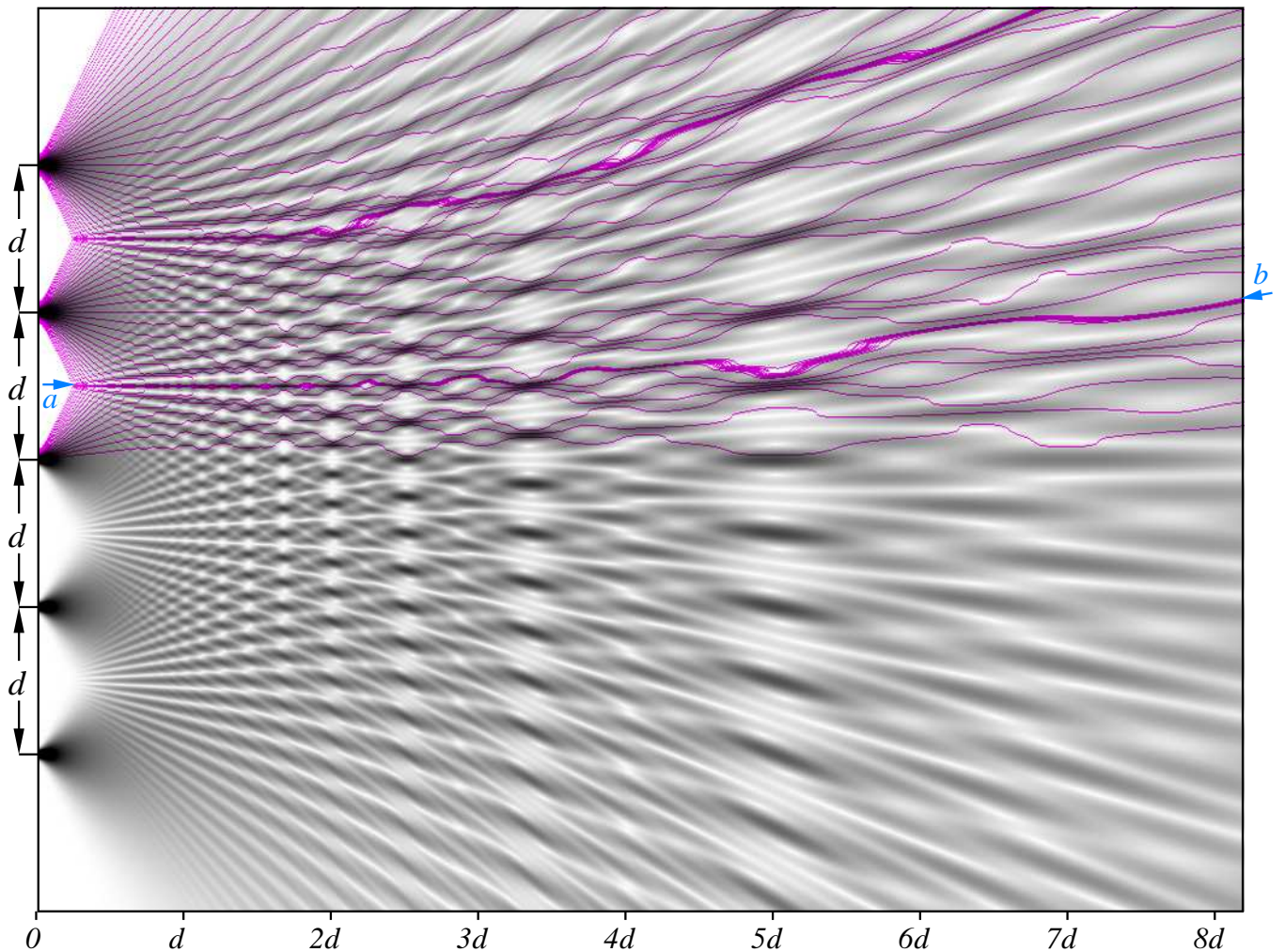


FIG. 7: Density distribution plot drawn by grey palette displays the Talbot effect: white color relates to zero intensity, and black color points to maximal intensity. Violet curves drawn in the upper part of the plot depict the bohmian trajectories. Distance  $d = 5 \times 10^{-8}$  m is equal to  $10 \cdot \lambda$ .

mines configuration of the wave function given in the working space. The function is named de Broglie pilot-wave [13]. In fact, its squared image, the density distribution 10, is shown in Fig. 7 in grey palette. So, the bohmian trajectory shows an optimal path for a particle, which is guided by the de Broglie pilot-wave within the working space.

## V. CONCLUDING DISCUSSION.

First of all, let us recall classical mechanics.

Geodesic trajectories in classical mechanics to be found by applying the principle of least ac-

tion [15] are real trajectories of mechanical objects. A beam of the trajectories, that tracks a relief, stems from the initial conditions slightly differing from each other. Observe that geodesic trajectories nowhere never intersect.

The number of trajectories, crossing a surface  $\delta S$ , is conserved, no matter how the surface deforms at moving along the beam. In fact, this observation demonstrates the conservation law of number of the trajectories passing through the surface, i.e., the trajectories never disappear and does not appear again. Violation of this law in classical physics would be tantamount to recognize teleportation - a classic body disappear suddenly and unexpectedly announced again.

Interpretation of the continuity equation of the density of trajectories is guided by incompressible fluid, which flows along routes specified by the geodesic trajectories. All physical space we can imagine is filled with this fluid [15, 16]. The basis for such an idealization is experience which shows, that there is a rather broad class of fluids for which even large changes in pressure do not lead to significant change in density. This fluid fills the environment continuously. Its molecular structure, at that, is ignored. In classical physics the continuity equation does not determine the fate of trajectories in the future. Their fate is determined only by the Hamilton-Jacobi equation. Other situation arises in quantum mechanics. Here the both equations, the continuity equation and the Hamilton-Jacobi equation, connected with each other via the bohmian quantum potential [8, 9], take part in determination of the geodesic trajectories.

In accordance with the de Broglie-Bohm interpretation, the wave function sets up a  $\Psi$ -field, which fills physical space of the experimental setup. Its squared modulus, the probability density distribution, is shown in Fig. 7, in gray palette. All physical space we can guess is filled by a fluid-like background with the density distribution  $|\Psi|^2$  [2, 17]. It is important to note, that the state of such a fluid is determined by geometry of the experimental setup. And route of the trajectories depends on the density of the fluid, its gradients, in the neighborhood of each point of the experimental setup. The guidance equation allows to find the trajectories that penetrate the field by the best way. In turn, the density distribution depends on the route of the trajectories. They are mutually dependent.

Such a fluid is seen to be vacuum. Polarization of vacuum is an extraordinary phenomenon since Hendrik Kasimir had proposed the existence of physical forces arising from a quantized field [18]. From this perspective, change of direction of a trajectory of a particle can be expressed in terms of exchange of virtual particles in vacuum. The vacuum has a vastly rich structure. It, implicitly, has all of the properties that a particle may have. This situation can be expressed by a sentence - the vacuum contains relative '*nothing*', and at the same time, the potential '*all*'.

The Feynman path integral [19] is a way to understand many manifestations of the vacuum. In fact, a proposition is as follows: virtual pairs emergent in a short time and annihilating in the end of the time loop are pairs permitting the particle to test a trajectory both forward and backward in time [20, 21, 22]. The extra degree of freedom obtained by allowing both directions in time gives the particle to get a non-local information needed for establishing an optimal path from a source to detector without the involvement of intelligent particles, intelligent observers, or multiple universes.

#### Acknowledgments

The author expresses his sincere thanks to Miss Pipa, the site administrator of Russian Quantum Portal, for developing and writing a program calculating the density distribution of the wave function at scattering on N-slit grating and bohmian trajectories outgoing from the slits. The results of this work are shown in Figs. 4, 6, and 7.

- 
- [1] A. D. Cronin, J. Schmiedmayer and D. E. Pritchard. Atom Interferometers, e-print URL <http://arxiv.org/abs/0712.3703v1>, (21 Dec 2007).
  - [2] M. Berry, I. Marzoli, and W. Schleich. Quantum carpets, carpets of light, Phys. World (6) (2001) 1-6.
  - [3] A. Steane. Quantum Computing, Rept. Prog. Phys. **61** (1998) 117-173.
  - [4] V. I. Sbitnev. Particle scattering on a N-slit screen: Talbot carpet and far-field diffraction, Kvantovaja magija **6**(1) (2009) 1101-1112, in Russian.
  - [5] M. M. Agamalyan, G. M. Drabkin, and V. I. Sbitnev. Spatial spin resonance of polarized neutrons. A tunable slow neutron filter, Phys. Rep. **168**(5) (1988) 265-303.
  - [6] A. S. Sanz and S. Miret-Artés. A causal look into the quantum Talbot effect, J. Chem. Phys. **126** (2007) 234106; e-print URL <http://arxiv.org/abs/quant-ph/0702224>, (19 Jun 2007).
  - [7] A. S. Sanz and S. Miret-Artés. A trajectory-based understanding of quantum interference, J. Phys. A: Math. Gen. **41** (2008) 435303; e-print URL <http://arxiv.org/>

- abs/0806.2105, (1 Oct 2008).
- [8] D. Bohm, A suggested interpretation of the quantum theory in terms of "Hidden Variables", *Phys. Rev.* **85** (1952) 166-193.
- [9] D. Bohm and B. J. Hiley. *The Undivided Universe: An ontological interpretation of quantum theory*, (Routledge, London, 1993).
- [10] G. I. Mark. Analysis of the spreading Gaussian wavepacket, *Eur. J. Phys.* **18** (1997) 247-250.
- [11] V. I. Sbitnev. Bohmian trajectories and the path integral paradigm. Complexified Lagrangian mechanics *IJBC*, **19**(7) (2009) xxxx-xxxx; e-print URL <http://arxiv.org/abs/0808.1245>, (8 Aug 2008).
- [12] M. Davidović, D. Arsenović, M. Božić, A. S. Sanz, and S. Miret-Artés. Should particle trajectories comply with the transverse momentum distribution?, *Eur. Phys. J. Special Topics* **160** (2008) 95, e-print URL <http://arxiv.org/abs/0803.2606>, (18 Mar 2008).
- [13] A. Valentini. De Broglie-Bohm Pilot-Wave Theory: Many Worlds in Denial? In: *Everett and his Critics*, eds. S. W. Saunders et al.. (Oxford, University Press, 2009), e-print URL <http://arxiv.org/abs/0811.0810>, (5 Nov 2008).
- [14] A. Kent. One world versus many: the inadequacy of Everettian accounts of evolution, probability, and scientific confirmation, In *Many Worlds? Everett, Quantum Theory and Reality*, eds. S. Saunders, J. Barrett, A. Kent and D. Wallace, O.U.P. upcoming, e-print URL <http://arxiv.org/abs/0905.0624>, (5 May 2009).
- [15] C. Lanczos. *The variational principles of mechanics*, (Dover Publ., Inc., N. Y. 1970).
- [16] R. E. Wyatt. *Quantum Dynamics with Trajectories: Introduction to Quantum Hydrodynamics*, (Springer, Berlin, 2005).
- [17] D. Bohm and J. P. Vigier. Model of the Causal Interpretation of Quantum Theory in Terms of a Fluid with Irregular Fluctuations, *Phys. Rev.* **96**(1) (1954) 208 - 216.
- [18] H. G. B. Casimir. On the attraction between two perfectly conducting plates, *Proc. Con. Ned. Akad. van Wetensch B51*(7) (1948) 793-796.
- [19] R. P. Feynman and A. Hibbs. *Quantum Mechanics and Path Integrals*, (McGraw Hill, N. Y. 1965).
- [20] G. N. Ord and R. B. Mann. Entwined pairs and Schrödinger's equation, *Annals of Physics*, **308**(2003) 478-492; e-print URL <http://arxiv.org/abs/quant-ph/0206095>, (14 Jun 2002).
- [21] G. N. Ord, J. A. Gualtieri, and R. B. Mann. A physical basis for the phase in Feynman path integration, e-print URL <http://arxiv.org/abs/quant-ph/0411005>, (31 Oct 2004).
- [22] P. J. Werbos and L. Dolmatova. The Backwards-Time Interpretation of Quantum Mechanics - Revisited With Experiment, e-print URL <http://arxiv.org/abs/quant-ph/0008036>, (7 Aug 2000).
- [23] [http://en.wikipedia.org/wiki/Talbot\\_effect](http://en.wikipedia.org/wiki/Talbot_effect)
- [24] [http://en.wikipedia.org/wiki/Thermal\\_neutron](http://en.wikipedia.org/wiki/Thermal_neutron)